View Online / Journal Homepage
Dynamic Article Links

Lab on a Chip

Cite this: DOI: 10.1039/c2lc21036c

www.rsc.org/loc

PAPER

Use of electrowetting to measure dynamic interfacial tensions of a microdrop

Riëlle de Ruiter,*[a] Peter Wennink,[a] Arun G. Banpurkar,[b] Michèl H. G. Duits[a] and Frieder Mugele[a]

Received 28th January 2012, Accepted 30th April 2012
DOI: 10.1039/c2lc21036c

Published on 30 May 2012 on http://pubs.rsc.org | doi:10.1039/C2LC21036C
Downloaded by Universiteit Twente on 01 June 2012

The adsorption of surface active species to liquid–liquid and to solid–liquid interfaces can have dramatic effects in microfluidics. In this paper we show how electrowetting on dielectric can be used to monitor a dynamic liquid–liquid interfacial tension (IFT) with a time resolution of $O(1\ s)$ using amplitude modulation of the AC voltage. This straightforward method, which requires less than a microlitre of sample, is demonstrated for aqueous drops containing Triton X-100 surfactant on a Teflon AF-coated substrate and with heptane as the immiscible oil ambient. Under these conditions, next to extracting the oil–water IFT (γ_{ow}), also the effective water–substrate IFT difference ($\Delta\gamma_{ws}$) can be obtained from the oil–water IFT and the Young's angle. Both γ_{ow} and γ_{ws} decrease over time due to adsorption. The measured dynamic oil–water IFT compares well to results of pendant drop experiments.

Introduction

Microfluidic systems are characterized by large surface-to-volume ratios. Interfacial tensions and their variation due to adsorption therefore play a key role for both the physical behaviour of the systems and for the performance of devices. This is particularly true for the increasingly popular digital microfluidic systems, which make use of small drops serving simultaneously as closed containers to manipulate the sample of interest and as microscopic reactors.[1–3] Especially, the analysis of physiological fluids like blood, urine, and saliva,[4] and of cultured pathogenic cells[5] increasingly find application. Frequently, such biochemical assays are based on reactions of the sample with ligands that are attached to the walls of the device.[6–9] Since most digital microfluidic systems make use of oil as an ambient medium (to prevent amongst others evaporation), good control and characterization of all interfaces including in particular the complex drop–(oil)–substrate interface is crucial. Several approaches have been implemented to measure IFTs in microfluidic systems.[10–16]

Electrowetting (EW) is arguably the most versatile technique to achieve detailed control over individual drops including all relevant operations such as drop formation, positioning, merging, mixing, and splitting.[17–20] EW relies on the balance of electrostatic forces acting on a conductive liquid drop in a non-conductive ambient medium with capillary forces resulting from the various interfacial tensions in the system. Since the electrostatic forces are determined exclusively by the geometry of both the drop and the electrodes, variations of the response of the drop to the electric fields as a function of time can be attributed to temporal variations of the interfacial tensions.

Previously, our group and others demonstrated that the EW response can be used to determine the equilibrium values of oil–water interfacial tensions for a variety of complex systems ranging from aqueous solutions of surfactants to milk.[21,22] It is shown that this method is especially suitable for small sample volumes, as opposed to conventional techniques, such as Wilhelmy plate, Du Noüy ring, and pendant drop tensiometry. More recently, this EW approach was adapted for measuring capacitance,[23] and for determining elastic moduli and extensional viscosities.[24,25]

In the present paper, we demonstrate a new method to monitor the temporal evolution of an oil–water interfacial tension due to the adsorption of surface active compounds by simply analysing the time-dependent EW response of sessile drops. Under the conditions used, one simultaneously obtains information about the complex drop–(oil)–substrate interface. The method is readily integrated into open digital microfluidic systems.[26] It offers a time resolution of a few seconds and is applicable for sample volumes down to approximately 20 nL. For the specific water-soluble surfactant under consideration here we find that the effective water–substrate interfacial tension varies in a very similar manner as the oil–water interfacial tension, which suggests the presence of a presumably molecularly thin oil film below the drop.

Materials and methods

A microscopic glass plate with a conductive indium tin oxide (ITO) layer is covered with a 3.5 μm thick layer of Teflon AF 1600 (DuPont), by twice dipcoating from a 3 wt% solution in FC-75 and heating in a vacuum oven. The thickness of the dielectric layer is determined in a calibration measurement with a

[a]*Physics of Complex Fluids, Faculty of Science and Technology, MESA+ Institute for Nanotechnology, University of Twente, P.O. Box 217, 7500 AE Enschede, The Netherlands. E-mail: r.deruiter-1@tnw.utwente.nl*
[b]*Center for Advanced Studies in Materials Science and Condensed Matter Physics, Department of Physics, University of Pune, Pune 411007, India*

Published on 30 May 2012 on http://pubs.rsc.org | doi:10.1039/C2LC21036C
Downloaded by Universiteit Twente on 01 June 2012

water drop in ambient silicone oil (Fluka), where the interfacial tension γ_{ow} is known to be 38 mN m^{-1}. Solutions of the nonionic surfactant Triton X-100 (Fluka) at 0.0005 and 0.001 wt% are prepared in ultrapure water (Millipore Synergy UV instrument, resistivity 18.2 MΩ cm). At those concentrations, which are well below the critical micelle concentration, the relaxation time of γ_{ow} due to adsorption is of O(10–100 s). KCl (Merck) was added to all aqueous phases to increase the conductivity to 3 mS cm^{-1}. Heptane (Fluka, γ_{ow} = 48 mN m^{-1}) was used as the ambient phase.

In the experiments, an aqueous drop of 10 μL is dispensed onto the substrate, while the system is submerged in the oil (Fig. 1a). Since the dispensing needle also serves as the electrical connection, the measurements can start within a few seconds after introducing the drop. We apply an electric field *via* a high frequency (10 kHz) carrier wave to avoid charge accumulation and to minimize possible effects of contact angle hysteresis.[27] The carrier wave is modulated with a low-frequency step profile, allowing to probe 5 (rms) voltages within each ramp (Fig. 1b). The total ramp time is varied between 2 to 25 s, while the discrete voltages U are distributed linearly between the square of the minimum (0) and maximum (50 V_{rms}). The time- and voltage-dependent contact angle θ (Fig. 1c) is recorded (and measured off-line) using an OCA 20L contact angle measuring and contour analysis system (DataPhysics). Dynamic oil–water IFTs extracted from these experiments are compared to measurements using the pendant drop technique.

Results and discussion

Fig. 2 illustrates the basic observation underlying our method: the contact angle of a drop decreases with increasing voltage as expected for electrowetting. However, the contact angle decrease is less pronounced for a freshly deposited drop (t = 0) than for an aged drop (t = 200 s). In contrast, the contact angle at zero voltage, *i.e.* Young's angle (θ_Y), appears to remain constant.

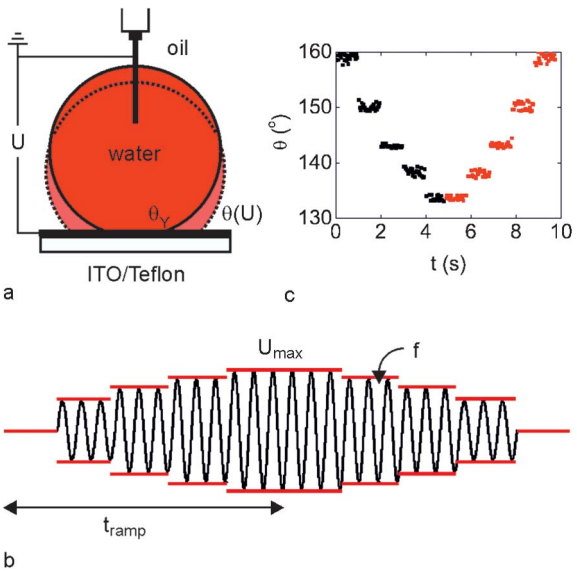

Fig. 1 Schematic showing (a) the electrowetting setup, (b) the applied signal (U_{max} = 50 V_{rms}, f = 10 kHz, t_{ramp} = 2, 5, 25 s), and (c) the corresponding stepwise changes in contact angle.

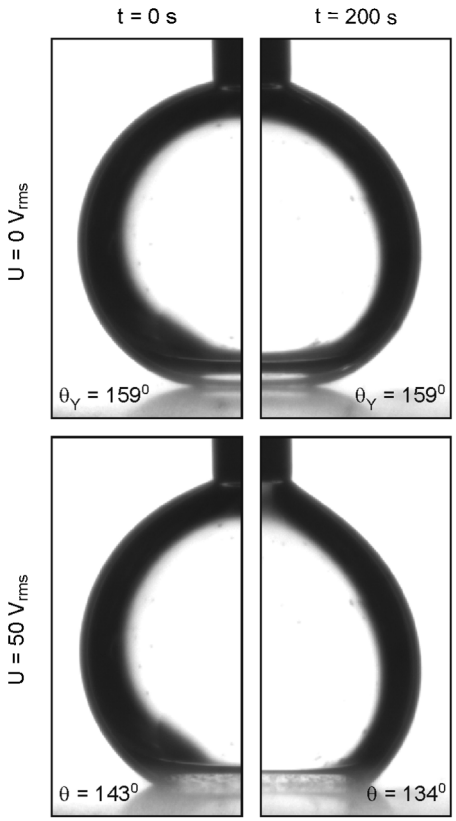

Fig. 2 Pictures showing the difference in contact angle without (top) and with (bottom) applied electric field, for a freshly deposited (left) and aged (right) aqueous drop with 0.001 wt% Triton X-100 in ambient heptane.

To analyse this behaviour in more detail, we deposit a drop onto the substrate (t = 0) and continuously ramp the voltage up and down (as in Fig. 1b). As illustrated by Fig. 3, cosθ increases proportionally with U^2, as expected based on the general electrowetting equation:[28]

$$\cos\theta(U) = \cos\theta_Y + \frac{C}{2\gamma_{ow}}U^2 \qquad (1)$$

where C represents the electric capacitance per unit area of the drop–substrate interface and is given by $C = \varepsilon_0\varepsilon_d/d$ with $\varepsilon_0\varepsilon_d$ the permittivity and d the thickness of the dielectric layer.† Over time, however, a gradual increase of the slope is observed; this can also be seen from the difference between subsequent ramps of increasing and decreasing voltage in Fig. 3. After approximately 10 cycles (of 5 s each) the variation of the slope saturates and the EW curve does not change anymore. Within the same time span, Young's angle $\theta(U = 0)$ hardly changes, as shown in the inset.

† Note that compared to the measurements of Ahmadi *et al.*[23] much smaller variations of the capacitance are expected in our system, as the thickness of the dielectric layer (3.5 μm) is orders of magnitude larger than the thickness of the adsorption layer and the entrapped oil layer.

This journal is © The Royal Society of Chemistry 2012

Published on 30 May 2012 on http://pubs.rsc.org | doi:10.1039/C2LC21036C
Downloaded by Universiteit Twente on 01 June 2012

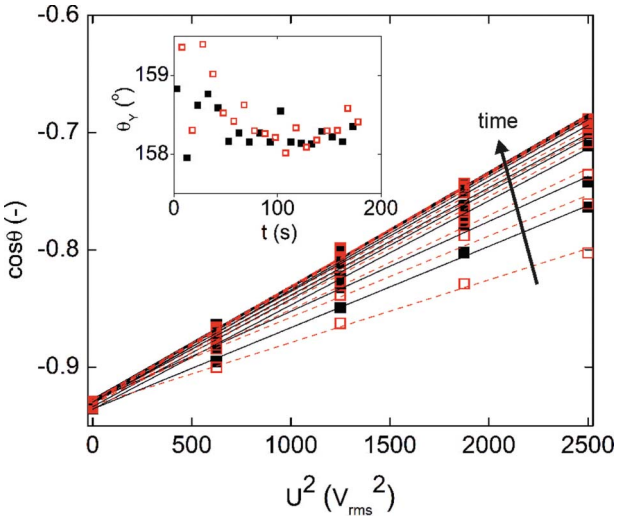

Fig. 3 Electrowetting curves for an aqueous drop with 0.001 wt% Triton X-100 in ambient heptane (t_{ramp} = 5 s), as determined for increasing (black, solid) and decreasing (red, open and dashed) voltage. The inset shows the evolution of the contact angle at 0 V, as extracted from the linear fits.

We now consider the time-dependence of our measurements in more detail. In general, the force balance at the three-phase contact line for a mechanically equilibrated drop reads:

$$\gamma_{ws}(t) + \gamma_{ow}(t)\cos\theta(U,t) = \gamma_{os}(t) + f_{el}(t) \qquad (2)$$

where $f_{el}(t) = CU(t)^2/2$ is the electrostatic force per unit length pulling on the contact line in the outward direction. In principle all interfacial tensions can vary over time, due to adsorption processes. The time dependence of the contact angle is the result of the slowly varying interfacial tensions $\gamma(t)$ in combination with the imposed $U(t)$ signal.

The data in Fig. 3 clearly demonstrate that there is a separation of time scales in the present experiments. On the one hand the drop responds quickly to variations of the amplitude of the applied (rms) voltage, on the other hand the interfacial tensions in the system slowly vary due to the adsorption of surfactant. Under these conditions, we can separate the EW response from the surfactant adsorption. For suitably chosen ramp times, the slope of each EW curve is determined exclusively by the momentary value of the oil–water interfacial tension. The increase in the slope of the EW curves with sample age then reflects the decrease of γ_{ow} with increasing surfactant adsorption. From a practical perspective, this implies that the ramp time must be chosen faster than the characteristic time for variations of the interfacial tension. The latter is related to the diffusion and/or adsorption time of the surfactant. If the ramp time is chosen too long we observe deviations from linearity in the ($\cos\theta$, U^2) relation (similar to Raccurt *et al.*[21]). For a typical drop size of the order of 10 μL, the hydrodynamic response time of the drop (O(10–50 Hz)) provides a lower limit of O(1 s) to the ramp time.

In Fig. 4a we make use of the separation of time scales to extract the oil–water interfacial tension as a function of time from the data in Fig. 3. We find that γ_{ow} decreases gradually, in an almost exponential manner. The first measurement point ($t \approx 0$) gives an IFT of 46 mN m^{-1}, which corresponds well with that of a pure heptane/water interface. This corroborates that the time used for introducing the drop and starting the experiment was short compared to the timescale for Triton X-100 adsorption at the oil–water interface. After a 'decay time' of about 60 s, γ_{ow} remains constant within 1%, an uncertainty that is also found in experiments with clean interfaces. We therefore assume that equilibrium has been reached.

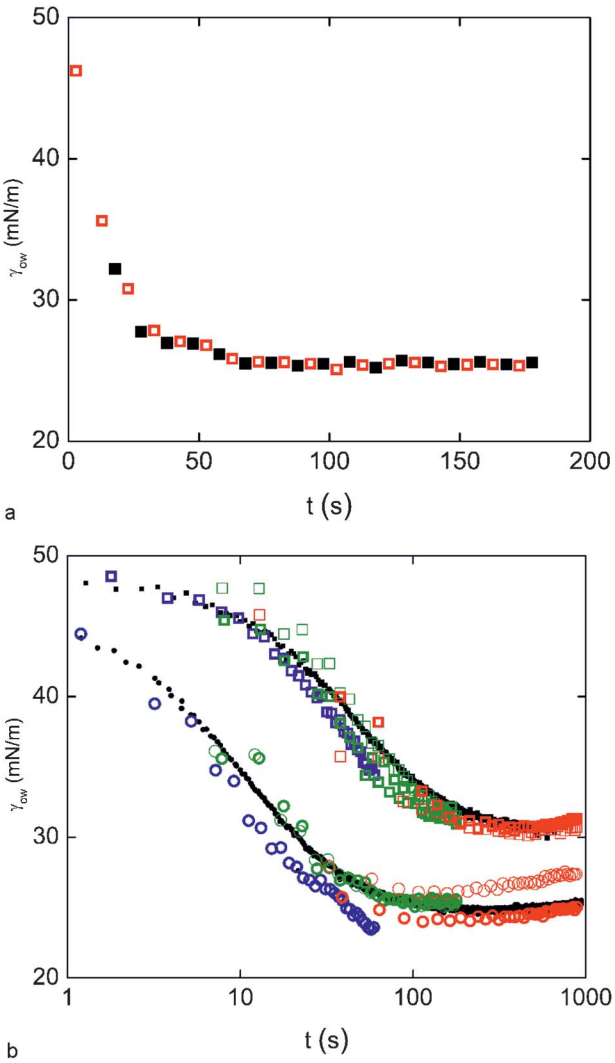

Fig. 4 Oil–water interfacial tension *versus* time for aqueous drops with Triton X-100 in ambient heptane. (a) Example for 0.001 wt% Triton X-100 (t_{ramp} = 5 s), as determined for increasing (black, closed) and decreasing (red, open) voltages. (b) Validation of electrowetting based tensiometry for various ramp times (2 s (blue), 5 s (green), and 25 s (red)) against pendant drop tensiometry (black) for Triton X-100 concentrations of 0.0005 wt% (squares) and 0.001 wt% (circles). Thick and thin symbols indicate duplicate measurements.

To validate these electrowetting-based results, we compare the extracted IFTs to pendant drop tensiometry measurements for the same concentrations of Triton X-100, see Fig. 4b. The shapes of the $\gamma_{ow}(t)$ curves agree well, and deviations between the two types of measurements are typically less than 5–10% (<3 mN m^{-1}). We consider this a good correspondence, taking into account the standard errors of both techniques, and small differences between

Published on 30 May 2012 on http://pubs.rsc.org | doi:10.1039/C2LC21036C
Downloaded by Universiteit Twente on 01 June 2012

the samples (like the geometry of the drop and its surroundings, and flow patterns inside the drops). It illustrates for the first time that also EW can be used to measure oil–water interfacial tensions with a time resolution of O(1 s).

From an applied perspective a few additional remarks can be made. Firstly, we note that our time resolution is enabled by choosing the voltages within the linear regime given by eqn (1). This is normally achieved by keeping $\Delta\cos(\theta) < 0.7$.[28] In this regime, sampling a straight line at 5 points offers an optimal trade-off between precision in IFT and resolution in time. After calibrating or calculating the capacitance C, the voltage range can be adjusted to the expected range of IFT values. Secondly, we note that EW-based tensiometry has distinct advantages when compared to pendant drop experiments. Unlike the latter method, EW does not require the Bond number to be above O(0.1).[29] Hence much smaller drops can be used, which is very useful when only tiny amounts of sample are available. This applies in the wire-drop geometry of the present study, and even more so in configurations with interdigitated EW electrodes. Another advantage of the low Bond number regime is that also systems with a small density difference between the drop phase and the ambient medium can be studied.

An additional capability of the EW-based method is that besides the oil–water interface, also the water–substrate interface can be characterized indirectly. After determination of γ_{ow} and θ_Y (independently) from the slope and intersection of the EW curve, eqn (2) can be used to determine $\gamma_{ws} - \gamma_{os}$. In the inset of Fig. 3 we showed that θ_Y is essentially constant throughout the present measurements. Since γ_{ow} decreases over time, $\gamma_{ws} - \gamma_{os}$ has to decrease as well (note that $\cos\theta_Y < 0$). The drop substrate interface may actually contain a thin film of a few layers of oil molecules separating the aqueous drop from the water repelling Teflon AF surface. Previous theoretical[30] and experimental[31] studies suggest the existence of such a layer in EW systems presumably due to a short-range repulsive component in the disjoining pressure. For the present system with a purely water-soluble surfactant and assuming no direct contact between the drop and the substrate, it is reasonable to assume that γ_{os} remains constant (see also Ahmadi *et al.*[23]). Based on this assumption we can extract the change in γ_{ws} from the variation of γ_{ow} and θ_Y with time. The results in Fig. 5 indeed indicate that γ_{ws} decreases in a very similar manner as γ_{ow}. In the present experiments, a few molecular layers of adsorbed oil might make the effective water–substrate interface 'look' similar to the oil–water interface for adsorbing Triton X-100 molecules. This rationalizes the similar trend for γ_{ws} and γ_{ow} in Fig. 5.

Note that a constant θ_Y is not required to extract $\Delta\gamma_{ws}$. The present situation is merely a specific case caused by the similar response in γ_{ws} and γ_{ow}. From an applied perspective, this situation is very desirable since it indicates that there is no excessive adsorption directly onto the solid surface. In fact, we find a very similar response for drops of cell medium in ambient silicone oil. Variations in the Young's angle over time are to be expected in experiments where the drop is in direct contact with the substrate, *e.g.* when air is used as the ambient phase. However, in that case additional pinning forces at the contact line introduce a (time-dependent) contact angle hysteresis, which complicates the experiments. As we can not exclude variations in the air–substrate IFT (γ_{vs}), the additional quantity that results from the combined analysis of γ_{ow} and θ_Y under such conditions is merely the difference $\gamma_{ws} - \gamma_{vs}$.

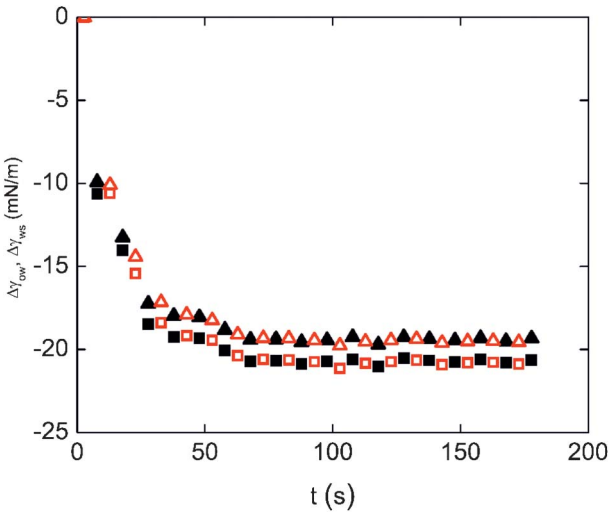

Fig. 5 Change in oil–water (squares) and water–substrate (triangles) interfacial tension *versus* time for aqueous drops with 0.001 wt% Triton X-100 in ambient heptane (t_{ramp} = 5 s), as determined for increasing (black, solid) and decreasing (red, open) voltages.

Conclusions

We demonstrated that time-resolved electrowetting in an open chip geometry can be used to measure the dynamic oil–water interfacial tension by analysing the variation in contact angle with the applied voltage as a function of drop age. In addition, information about the complex drop–(oil)–substrate interface can be obtained. In the measurement strategy it is assumed that the drop's response to a voltage change occurs in a much shorter time than the characteristic adsorption time of the surfactant. Typical processes that can be resolved have a relaxation time of O(10 s) and involve interfacial tension changes by more than 10%.

Besides yielding more than one IFT, our method also has the advantage that it requires neither a density difference between the fluid phases, nor drop sizes of O(1 mm). Although not explicitly shown here it is obvious that the method can be implemented in wireless configurations using an EW single surface with interdigitated electrodes.[22] Next to integration into single-surface EW devices[26,32] this also enables the analysis of sample volumes down to 20 nL or less.

References

1 S. Y. Teh, R. Lin, L. H. Hung and A. P. Lee, *Lab Chip*, 2008, **8**, 198–220.
2 M. Abdelgawad and A. R. Wheeler, *Adv. Mater.*, 2009, **21**, 920–925.
3 M. J. Jebrail and A. R. Wheeler, *Curr. Opin. Chem. Biol.*, 2010, **14**, 574–581.
4 V. Srinivasan, V. K. Pamula and R. B. Fair, *Lab Chip*, 2004, **4**, 310–315.
5 I. Barbulovic-Nad, H. Yang, P. S. Park and A. R. Wheeler, *Lab Chip*, 2008, **8**, 519–526.
6 J. Y. Yoon and R. L. Garrell, *Anal. Chem.*, 2003, **75**, 5097–5102.
7 A. Bange, H. B. Halsall and W. R. Heineman, *Biosens. Bioelectron.*, 2005, **20**, 2488–2503.

 This journal is © The Royal Society of Chemistry 2012

8 M. D. Goldberg, R. C. Lo, S. Abele, M. Macka and F. A. Gomez, *Anal. Chem.*, 2009, **81**, 5095–5098.
9 A. H. C. Ng, U. Uddayasankar and A. R. Wheeler, *Anal. Bioanal. Chem.*, 2010, **397**, 991–1007.
10 S. D. Hudson, J. T. Cabral, W. J. Goodrum, K. L. Beers and E. J. Amis, *Appl. Phys. Lett.*, 2005, **87**, 081905.
11 J. T. Cabral and S. D. Hudson, *Lab Chip*, 2006, **6**, 427–436.
12 N. T. Nguyen, S. Lassemono, F. A. Chollet and C. Yang, *IEE Proc.: Nanobiotechnol.*, 2006, **153**, 102–106.
13 J. H. Xu, S. W. Li, W. J. Lan and G. S. Luo, *Langmuir*, 2008, **24**, 11287–11292.
14 K. Wang, Y. C. Lu, J. H. Xu and G. S. Luo, *Langmuir*, 2009, **25**, 2153–2158.
15 M. L. J. Steegmans, A. Warmerdam, K. G. P. H. Schroen and R. M. Boom, *Langmuir*, 2009, **25**, 9751–9758.
16 H. Gu, M. H. G. Duits and F. Mugele, *Colloids Surf., A*, 2011, **389**, 38–42.
17 M. G. Pollack, A. D. Shenderov and R. B. Fair, *Lab Chip*, 2002, **2**, 96–101.
18 S. K. Cho, H. J. Moon and C. J. Kim, *J. Microelectromech. Syst.*, 2003, **12**, 70–80.
19 R. B. Fair, *Microfluid. Nanofluid.*, 2007, **3**, 245–281.
20 F. Mugele, M. Duits and D. van den Ende, *Adv. Colloid Interface Sci.*, 2010, **161**, 115–123.
21 O. Raccurt, J. Berthier, P. Clementz, M. Borella and M. Plissonnier, *J. Micromech. Microeng.*, 2007, **17**, 2217–2223.
22 A. G. Banpurkar, K. P. Nichols and F. Mugele, *Langmuir*, 2008, **24**, 10549–10551.
23 A. Ahmadi, K. D. Devlin, H. Najjaran, J. F. Holzman and M. Hoorfar, *Lab Chip*, 2010, **10**, 1429–1435.
24 A. G. Banpurkar, M. H. G. Duits, D. van den Ende and F. Mugele, *Langmuir*, 2009, **25**, 1245–1252.
25 W. C. Nelson, H. P. Kavehpour and C.-J. C. Kim, *Lab Chip*, 2011, **11**, 2424–2431.
26 M. Abdelgawad, S. L. S. Freire, H. Yang and A. R. Wheeler, *Lab Chip*, 2008, **8**, 672–677.
27 F. Li and F. Mugele, *Appl. Phys. Lett.*, 2008, **92**, 244108.
28 F. Mugele and J. C. Baret, *J. Phys.: Condens. Matter*, 2005, **17**, R705–R774.
29 N. J. Alvarez, L. M. Walker and S. L. Anna, *J. Colloid Interface Sci.*, 2009, **333**, 557–562.
30 C. Quilliet and B. Berge, *Europhys. Lett.*, 2002, **60**, 99–105.
31 A. Staicu and F. Mugele, *Phys. Rev. Lett.*, 2006, **97**, 167801.
32 U. C. Yi and C. J. Kim, *J. Micromech. Microeng.*, 2006, **16**, 2053–2059.

Published on 30 May 2012 on http://pubs.rsc.org | doi:10.1039/C2LC21036C
Downloaded by Universiteit Twente on 01 June 2012